Deformation and toughness of polymeric systems: 4. Influence of strain rate and temperature

M. C. M. van der Sanden* and H. E. H. Meijer†
Centre for Polymers and Composites (CPC), Eindhoven University of Technology, PO Box 513, 5600 MB Eindhoven, The Netherlands
(Received 2 June 1993; revised 3 December 1993)

The influence of testing speed and temperature on the brittle-to-tough transition of non-adhering core–shell rubber-modified polystyrene–poly(2,6-dimethyl-1,4-phenylene ether) (PS-PPE) blends was studied. The validity of the concept of a network density dependent, critical matrix ligament thickness (ID_c, as introduced in this series and verified mainly by slow-speed uniaxial tensile testing) is demonstrated for notched high-speed (1 m s^{-1}) tensile testing at different temperatures. The influence of testing speed and temperature on the absolute value of ID_c can be quantitatively understood in terms of a strain rate and temperature dependence of the yield stress. The simple model introduced in part 2 of this series proves to be valid under all testing conditions studied varying from temperatures of 50 to 150°C below the glass transition temperature of the PS-PPE blends. The absolute value of the tensile toughness, on the contrary, is a not yet quantified function of the test geometry applied and, consequently, cannot be directly derived from a simple strain-to-break argument.

(Keywords: deformation; toughness; network density)

INTRODUCTION

In part 1 of this series[1] the concept of a material-specific critical thickness (ID_c) was introduced using (macroscopically) brittle polystyrene (PS). It was demonstrated that a control of the microstructure allowed for an increase of the macroscopic draw ratio (λ_{macr}) from 1 to 60% of the theoretical natural draw ratio (λ_{max}) based on the maximum extension of a single strand of the molecular network structure. In part 2[2] the influence of the physical network structure of the polymeric material on the value of ID_c was investigated using the homogeneously miscible system polystyrene–poly(2,6-dimethyl-1,4-phenylene ether) (PS-PPE), while in part 3[3] crosslinked epoxides were used to extend the concept to chemical networks.

In the systems with a high network density, notably all chemical networks of part 3, the critical ligament thickness could only be determined using relatively extreme testing conditions, i.e. notched high-speed (1 m s^{-1}) tensile testing at different temperatures. Nevertheless, all data concerning ID_c obtained under different testing conditions were plotted in one graph and compared with the predictions derived from the simple, energy-based model as proposed in part 2. In this study we try to find experimental evidence for this generalization of the basic concept. In particular, the influence of testing speed and temperature on the absolute value of ID_c will be studied.

The expression for ID_c is given in equation (1)[2]:

$$ID_c = \frac{6(\gamma + k_1 \nu^{1/2})E_1}{k_2 \nu^{-1/2} \sigma_y^2} \tag{1}$$

where γ is the van der Waals surface energy, k_1 and k_2 are constants ($k_1 = 7.13 \times 10^{-15}$ J chain$^{-1/2}$ m$^{-1/2}$ and $k_2 = 2.36 \times 10^{13}$ chains$^{1/2}$ m$^{-3/2}$) (ref. 2), ν is the network density (entanglement and/or crosslink density), E_1 is the Young's modulus and σ_y is the yield stress. Inspection of equation (1) reveals that to a first approximation the yield stress is the only parameter demonstrating a strong strain rate and temperature dependence below the glass transition temperature (T_g) of the polymer. [The temperature and strain rate dependence of the Young's modulus is neglected to a first approximation, although its temperature and strain rate dependence is in general comparable with the temperature and strain rate dependence of the yield stress. However, the yield stress is more dominant in equation (1).] Applying the Eyring theory of viscosity[4] the strain rate and temperature dependence of the yield stress can be described as:

$$\dot{\varepsilon} = A_E \exp\left[-\frac{(\Delta E^* - V^* |\sigma_y|)}{RT} \right] \tag{2}$$

where $\dot{\varepsilon}$ is the strain rate, A_E is a constant, ΔE^* is the activation energy, V^* is the activation volume, R is the gas constant and T is the absolute temperature. Equation (2) suggests a linear relationship between yield stress and absolute temperature and a logarithmic dependence of the yield stress on the strain rate. Combining equations (1) and (2) results in a description of the strain

* Present address: Physics Department, University of California at Santa Barbara, Broida Hall, Santa Barbara, CA 93106, USA
† To whom correspondence should be addressed

0032-3861/94/13/2774–09

rate and temperature dependence of ID_c. In *Figure 1* the predicted values of ID_c are shown as a function of temperature, strain rate and network density.

The constants in equation (2) are extracted from literature data[5] of the yield stress at very low strain rates at room temperature combined with data determined in our laboratory[6]. For simplification it is assumed that the strain rate dependence of the yield stress is independent of the PS-PPE composition and that the temperature dependence, $(T_g - T)$, of the yield stress is independent of the network density†. From *Figure 1a* it is clear that the critical thickness (for PS-PPE 100-0 as well as for 20-80) increases with a decreasing strain rate and increasing temperature. The planes shown in *Figure 1a* intersect at higher temperatures due to the fact that the T_g of PS (88°C) is much lower than that of the 20-80 blend (174°C). *Figure 1b* clearly reveals the influence of temperature of the value of the critical thickness: slightly dependent on the strain rate applied, the value of ID_c strongly increases, within the region of $0 < (T_g - T) < 25$°C, if the glass transition is approached. From *Figure 1c*, finally, it can be inferred that the strain rate dependence of ID_c is only significant if the material is strained close to the T_g. The network density dependence, as already extensively discussed in part 2 of this series[2], is obvious in both *Figures 1b* and *c*.

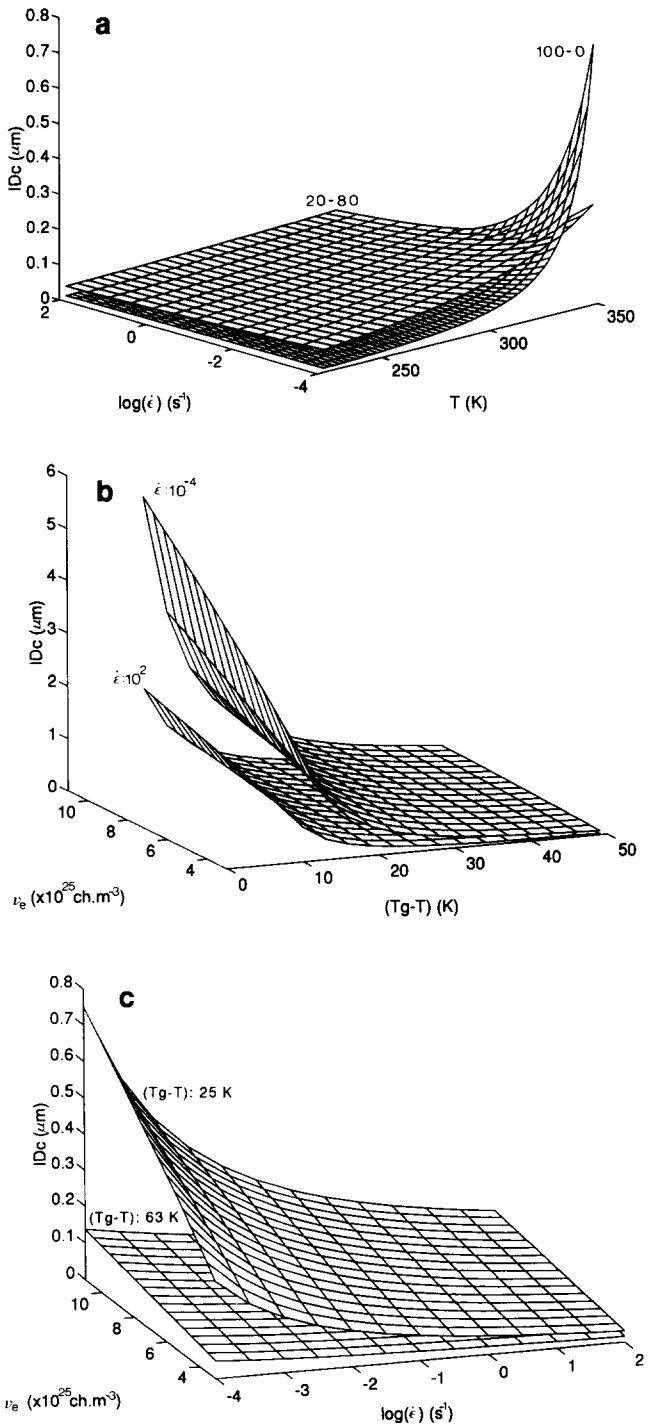

Figure 1 Predicted values of the critical matrix ligament thickness as a function of temperature, strain rate and network density: (a) PS-PPE 100-0 and 20-80; (b) $\dot{\varepsilon} = 10^{-4}\,s^{-1}$ and $\dot{\varepsilon} = 10^{2}\,s^{-1}$; and (c) $(T_g - T) = 25$ K and $(T_g - T) = 63$ K

This study provides the experimental verification of the strain rate and temperature dependence of ID_c using the PS-PPE model system. The values of the critical ligament thickness as determined by uniaxial slow-speed tensile testing at room temperature[2] are compared with those obtained by notched high-speed tensile testing ($1\,m\,s^{-1}$) at different temperatures. In order to complete the analysis, high-speed dilatometry ($1\,m\,s^{-1}$; strain rate $10\,s^{-1}$) is used to reveal the change in deformation mechanism from (multiple) crazing to shear deformation at the ID_c.

EXPERIMENTAL

Materials

The materials used were (identical to ref. 2) PS (Dow, Styron 638), PPE (General Electric Co., PPE-803) and the core–shell rubber with a poly(methyl methacrylate) shell and a styrene–butadiene core (Rohm and Haas Co., Paraloid EXL 3647). The core–shell rubber was an extrusion grade and contained 11 wt% poly(methyl methacrylate). The core–shell rubber particle size was in the range of 0.1–0.3 μm.

Sample preparation

The PS-PPE compounding was carried out as extensively described in part 2 of this series[2]. Neat PS-PPE blends were prepared via a double extrusion cycle either by diluting a PS-PPE 50-50 master-batch with PS (PS-PPE 80-20 and 60-40 blends) or by direct mixing of PS and PPE (100-0, 40-60 and 20-80 blends). Rubber-modified PS-PPE blends with different compositions: 10, 20, 30, 40, 50 and 60 wt% non-adhering core–shell rubber were prepared via the same two-step compounding process with the addition of the core–shell rubber in the second extrusion step (processing temperatures: see ref. 2). Blend compositions are indicated with a three number code: A-B/C, where A is the weight fraction of PS present in the matrix, B is the weight fraction of PPE present in the matrix and C is the weight fraction of core–shell rubber present in the total blend.

† The constants used to calculate *Figure 1a* are for PS: $V^* = 5.46 \times 10^{-4}$ $m^3\,mol^{-1}$, $\Delta E^* = 251\,kJ\,mol^{-1}$ and $\log A_E = 32$; and for PS-PPE 20-80: $V^* = 5.46 \times 10^{-4}\,m^3\,mol^{-1}$, $\Delta E^* = 133\,kJ\,mol^{-1}$ and $\log A_E = 11$. *Figures 1b* and *c* are based on the constants as listed above for PS, combined with the assumption that the yield stress is independent of the network density

Extruded strands were quenched in a water bath and pelletized subsequently. High-speed dilatometry specimens were prepared by injection moulding (Arburg Allrounder 220-75-250) the blends into dog-bone-shaped tensile bars (DIN 53 455, sample thickness: 3 mm). Square plates (length × width × thickness: 60 × 60 × 3 mm) were injection moulded at temperatures depending on the blend composition[2]. Parallel to the direction of injection moulding specimens were machined with dimensions (length × width × thickness): 60 × 10 × 3 mm. Analogous to the Izod impact test protocol (ASTM D256) the bars were V-shaped single-edge notched in the centre (notched high-speed tensile specimens).

Mechanical testing

Prior to mechanical testing the injection-moulded and machined specimens were annealed at a temperature 20°C below the T_g of the matrix for 24 h.

In part 1 of this series[1] tensile dilatometry has revealed its use to determine the deformation mechanisms of PS. Here, tensile dilatometry has been carried out at 1 m s^{-1} (strain rate 10 s^{-1}) on the unnotched samples using two contactless electro-optical displacement transducers (EODT: Zimmer type 100D; lenses: model 100-02, 2 mm range). The EODT converts the motion of a black and white edge (target) into a voltage proportional to the displacement in the frequency range from 0 to 400 kHz. Using two EODTs positioned at the edges of the white-painted rectangular part (middle section) of the dog-bone-shaped sample, the absolute displacements of the two edges of the sample could be registered. Assuming that the relative displacement of the sample in both directions perpendicular to the load direction is equal, the transverse change in cross-sectional area could be recorded. The longitudinal strain was obtained from the cross-head displacement of the tensile machine (type Zwick Rel SB 3122). Hence, the volume–strain could be obtained from these measurements as a function of the longitudinal strain.

High-speed impact testing is performed by uniaxial straining of single-edge notched specimens at 1 m s^{-1}. High-speed notched impact toughness (G_h; 1 m s^{-1}) is defined as: the energy absorbed (i.e. integrated area under the stress–strain curve) during fracture of a single-edge notched (razor-blade tapped) tensile specimen over the original area behind the crack-tip (see ref. 3 for a detailed description of the test). The free sample length between the clamps was 20 mm. Impact testing was performed within the range of −75°C to 80°C on a Zwick Rel SB 3122 tensile machine equipped with a climate chamber. At least five specimens were fractured for each testing condition in order to obtain an average value of G_h.

Table 1 Entanglement molecular weight (M_e) and entanglement density (ν_e) of neat PS-PPE blends

Blend composition (PS-PPE)	M_e (kg mol^{-1})	ν_e ($\times 10^{25}$ chains m^{-3})
100-0	20	3
80-20	12	5
60-40	8.6	7
40-60	6.7	9
20-80	5.5	11

RESULTS AND DISCUSSION

The determination of the molecular weight between entanglements (M_e) and entanglement density (ν_e) of the various PS-PPE blends from dynamic mechanical thermal analysis has already been described in part 2 of this series[2]. In *Table 1* the values of M_e and ν_e are recapitulated.

Unnotched samples

In *Figure 2* the true stress and relative volume change of core–shell rubber-modified pure PS as measured at 1 m s^{-1} (strain rate 10 s^{-1}) is shown as a function of the longitudinal strain. Similar to the slow-speed tensile dilatometry results[1], PS containing up to 50 wt% non-adhering core–shell rubber demonstrates a typically brittle deformation behaviour although the stresses are somewhat increased due to the higher strain rates applied. The slope of the relative volume change *versus* strain curve is close to unity, indicating a deformation process accompanied by void formation. This void formation can be attributed either to crazing or to the process of particle/interface detachment. Tensile dilatometry cannot distinguish between those two processes. If, however, the rubber content is increased to 60 wt% the true stress–strain curve shows the characteristics of a true yield point followed by a constant stress level. Also the slope of the relative volume change *versus* strain curve deviates from unity and decreases to zero. The latter implies that a shear deformation process occurs in this system. Similar to the slow-speed tensile dilatometry results on core–shell rubber-modified PS the brittle-to-ductile transition is located between 50 wt% rubber and 60 wt% rubber (thus $ID_c \sim 0.05$ μm) for pure PS. At this transition the deformation mechanism changes from crazing to shearing apparently irrespective of the strain rate applied, illustrating the strain rate insensitivity of the value of the ID_c in the region of low network (entanglement) densities within the investigated strain rate range (the temperature and strain rate sensitivity of ID_c will be discussed more extensively in the next section). However, the macroscopic strain-to-break of the shear deforming PS system is only ~80% (not shown in *Figure 2*), compared to 200% for the slow-speed analysis[1],

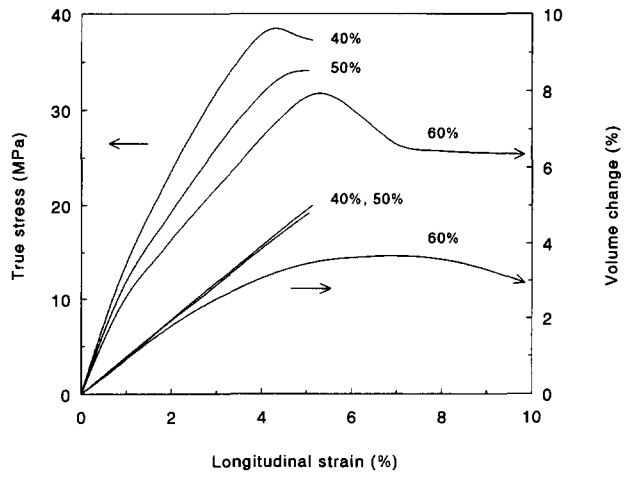

Figure 2 Stress–strain and volume–strain curves of rubber-modified PS blends tested at 1 m s^{-1} (strain rate 10 s^{-1}) for the rubber contents indicated

indicating that ID_c has just been surpassed by the addition of 60 wt% core–shell rubber. Apparently, the local strain rate in the matrix ligament is only slightly influenced by the macroscopically applied strain rate. [Increasing the macroscopically applied strain rate from 8.3×10^{-4} (i.e. 5 mm min^{-1}) up to 10 s^{-1} (i.e. 1 m s^{-1}) does not result in a complete brittle fracture of the material as expected from the decrease of ID_c from 0.05 to 0.025 μm (based on *Figure 1a*, $T = 298$ K, or see equations (1) and (2)).]

Notched samples

Tensile toughness data. In *Figure 3* the influence of temperature on the value of ID_c at notched high-speed tensile testing conditions is shown for the various PS-PPE

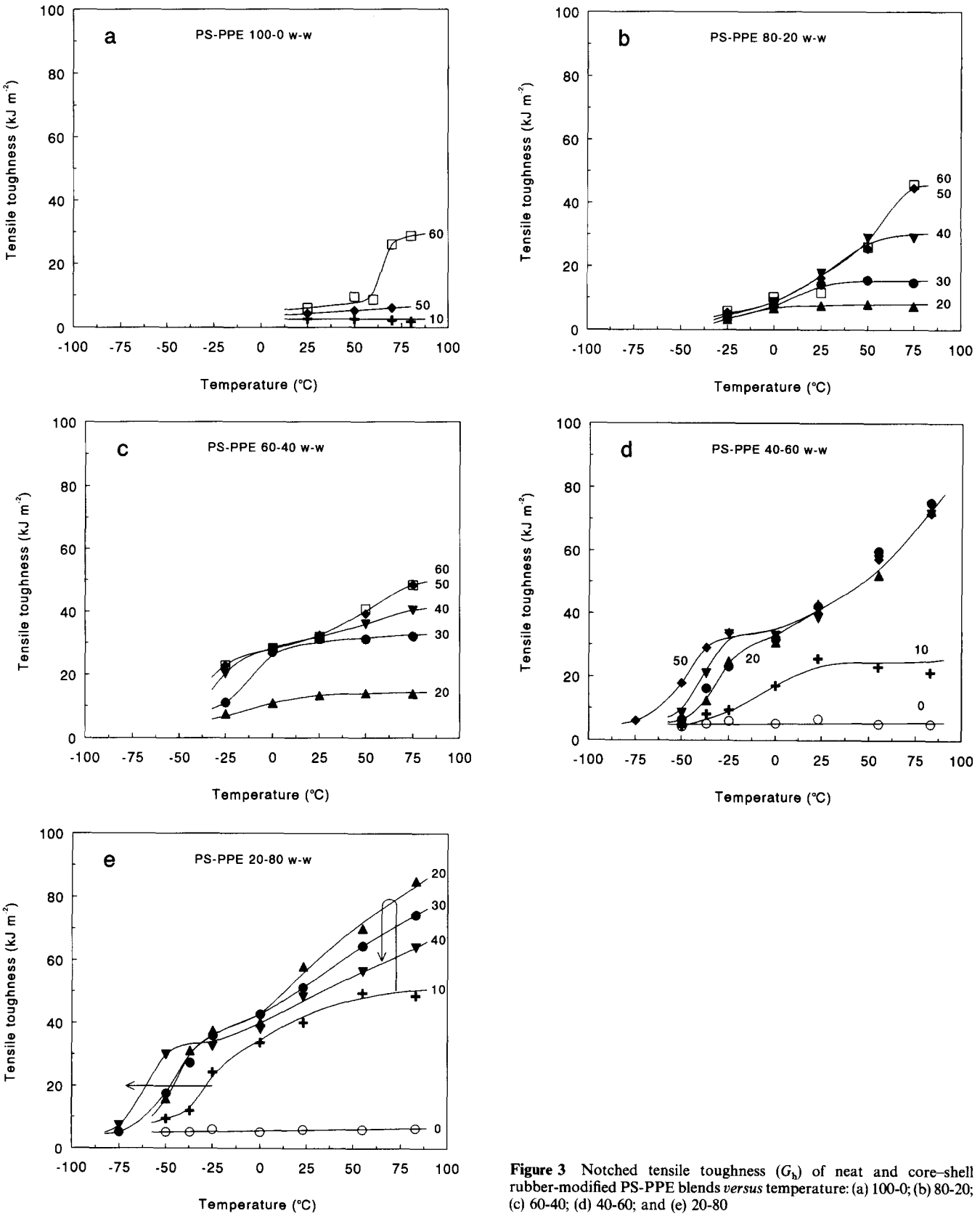

Figure 3 Notched tensile toughness (G_h) of neat and core–shell rubber-modified PS-PPE blends *versus* temperature: (a) 100-0; (b) 80-20; (c) 60-40; (d) 40-60; and (e) 20-80

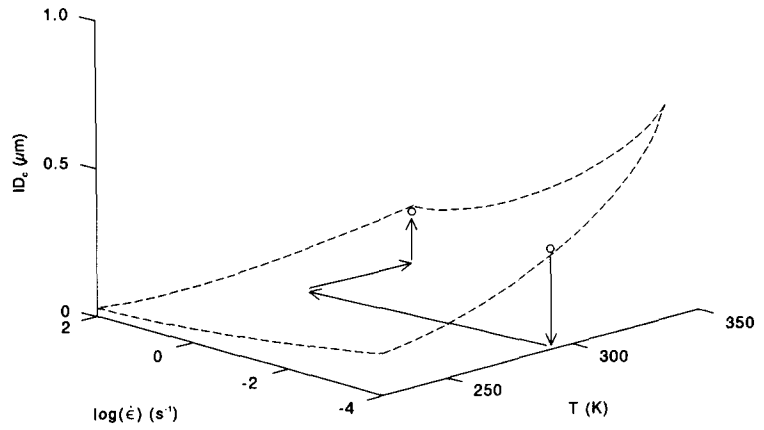

Figure 4 Schematic representation of the influence of temperature and strain rate on the critical matrix ligament thickness

blends filled with different amounts of non-adhering core–shell rubber. Rubber-modified PS only demonstrates a brittle-to-ductile transition at 60 wt% rubber close to the T_g of the PS matrix (88°C; *Figure 3a*). Analogous to the value of ID_c as found in slow-speed[1] and high-speed unnotched uniaxial tensile testing at room temperature (*Figure 2*) the brittle-to-tough transition of core–shell rubber-modified PS is found to be at 0.05 μm for notched high-speed impact testing but now at a temperature of 70°C. Apparently, the introduction of a notch has increased the local strain rate (and, consequently, the value of the yield stress) such that an increase in temperature to 70°C is required to keep $ID_c \approx 0.05$ μm (*Figure 4*). In *Figure 3b* the notched high-speed impact toughness of the PS-PPE 80-20/*X* blends is shown. Blends containing <20 wt% core–shell rubber are omitted for the sake of simplicity; these materials demonstrate a brittle fracture behaviour in the entire temperature range investigated. Taking 75°C as a reference temperature it can be concluded that upon increasing the rubber concentration the tensile toughness increases. However, increasing the rubber content from 50 to 60 wt% does not result in a further increase of the absorbed energy during notched high-speed fracturing of the sample. Hence, the brittle-to-tough transition of the PS-PPE 80-20 blend at 75°C is located at 0.06 μm. Slow-speed uniaxial tensile testing resulted in the same value of the ID_c at room temperature[2]. As expected (see Introduction: *Figure 1b* and the discussion of *Figure 3a*), the increase of the yield stress as a consequence of the high speed occurring locally at the notch-tip is counteracted by the increased temperature at which the brittle-to-ductile transition is observed. With increasing temperature the tensile toughness of the 80-20/60 blend increases continuously within the temperature range investigated. This is also reflected in the increased size of the whitened area above and below the fracture surface of the 80-20/*X* blends with increasing testing temperature (not shown here).

Increasing the PPE content of the matrix (*Figure 3c*) results in a confirmation of the trends discussed above. For the PS-PPE 60-40 blend the value of the ID_c at 75°C is positioned around 0.07 μm (corresponding to 50 wt% core–shell rubber). At lower temperatures a brittle-to-ductile transition cannot be determined due to the fact that no significant distinction can be made between the different levels of tensile toughness.

Figure 3d shows the results of the PS-PPE 40-60/*X* blends. At 75°C the brittle-to-tough transition is located between 10 wt% and 20 wt% core–shell rubber (~0.17 μm, assuming that the critical concentration is close to 20 wt% core–shell rubber) since an increase of the rubber concentration (up to 50 wt%) does not result in a higher value of the tensile toughness. Inspection of *Figure 1b* reveals that a brittle-to-ductile transition can also be observed as a function of temperature at a constant value of the matrix ligament thickness (i.e. rubber concentration). For example the 50 wt% core–shell rubber-modified PS-PPE blend (40-60/50) shows a brittle-to-tough transition temperature (T_{BT}) of ~ −50°C (*Figure 3d*). Increasing the average matrix ligament thickness, by decreasing the rubber content, results in an increase of the brittle-to-ductile transition temperature.

The PS-PPE 20-80/*X* blends demonstrate a clear deviation from the general aspects as discussed above (*Figure 3e*). At 75°C the brittle-to-ductile transition is located between 10 wt% and 20 wt% core–shell rubber ($ID_c = 0.22$ μm, assuming that the critical condition is located close to the 10 wt% rubber-modified PS-PPE blend). Increasing the rubber content above 20 wt% results in a decrease of the tensile toughness at this temperature. Hence, the level of tensile toughness decreases after passing the brittle-to-tough transition. The origin of this decrease is illustrated in *Figure 5* which shows the recorded force–time traces of the various PS-PPE 20-80/*X* blends at 75°C. Clearly the time-to-failure (read 'strain-to-break') continuously increases with an increasing rubber content. The maximum stress on the other hand increases only if the rubber concentration is increased from 0 to 10 wt%, but decreases upon extra rubber addition. Since the tensile toughness shown in *Figures 3a–e* is correlated with the surface area under the recorded force–time traces (energy), it is clear that the decrease in maximum force upon increasing the rubber content after passing the T_{BT}, is not fully compensated for by the increased time-to-failure (read 'strain'). A higher rubber concentration at the brittle-to-tough transition automatically results in a decrease of the macroscopic force of the recorded force–time trace since more 'holes' are present in the material. Consequently, with an increasing rubber concentration an optimum can be observed for the tensile toughness value after passing the brittle-to-tough transition, partly due to an overlap of

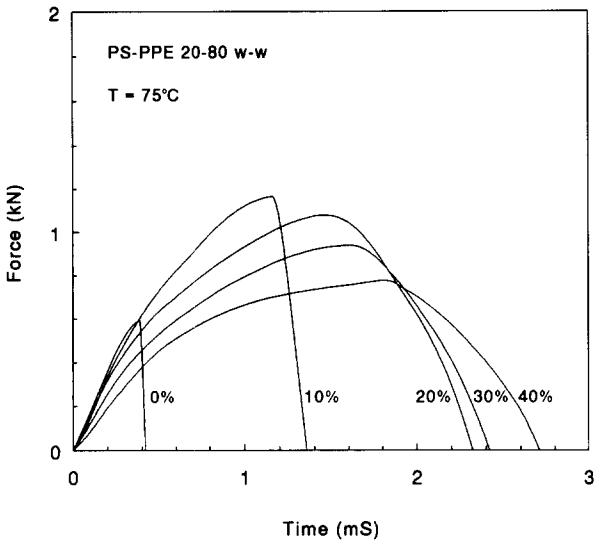

Figure 5 Force–time traces of rubber-modified 20-80 blends recorded at 75°C

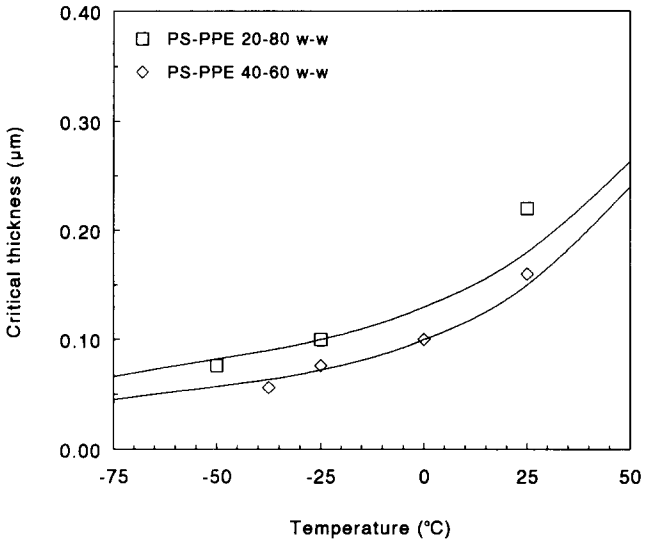

Figure 6 Critical matrix ligament thickness *versus* temperature for two rubber-modified PS-PPE blends (40-60 and 20-80). The full curves are according to the model

stress fields[7,8]. Macroscopically, this results in a decrease of the recorded forces (stresses). In conclusion, the simple network density dependent strain-to-break argument postulated in part 1 of this series results in conclusive data with respect to the value of the critical interparticle distance but cannot fully account for the network density dependence of the measured value of the notched tensile toughness. Only detailed micromechanical modelling can provide quantitative answers. This aspect is one of the topics of the present research at our laboratory.

In *Figure 6* the temperature dependence of the ID_c is shown for the PS-PPE 40-60 and 20-80 blends (cf. *Figures 3d* and *e*). The theoretical curves of the critical ligament thickness are calculated using yield stress data at room temperature[5] (irrespective of the different strain rates applied) and assuming a linear relationship with temperature to a final value of zero at the T_g. [From *Figure 1* it is clear that the strain rate dependence of ID_c is rather weak, except close to the T_g. Hence, it appears justified to use yield stress data available in the literature[5] from slow-speed tensile tests (strain rate $10^{-4}\,s^{-1}$) in order to calculate ID_c as a function of temperature for the notched high-speed tensile specimens.] The full curves in *Figure 6*, consequently, represent a cross-section in *Figure 1b* at constant strain rate ($10^2\,s^{-1}$; an estimated strain rate behind the notch-tip of the notched high-speed impact samples). From *Figure 6* it can be inferred that the temperature dependence of ID_c can be predicted satisfactorily for two of the investigated PS-PPE blends applying the simple model presented in part 2 of this series[2] in combination with an Eyring activated flow process despite the fact that the local yield stress in a matrix ligament cannot be simply related to a macroscopic yield stress due to the presence of a notch (see discussion of *Figure 3a*).

Visualization of the deformation process. To gain more insight into the deformation process occurring in front of the crack-tip during notched tensile testing in the ductile region micrographs were taken at several stages of the process. Since the PS-PPE 20-80/X (for $X > 10$) blends already demonstrate the characteristics of a ductile fracture during notched high-speed tensile testing at room temperature (*Figure 3e*) these blends will certainly reveal ductile fracture during slow-speed notched tensile testing (cf. *Figure 1a*). In *Figure 7* the deformation process of a PS-PPE 20-80/30 blend is illustrated as observed in the ductile region during a slow-speed notched tensile test ($5\,mm\,min^{-1}$) at room temperature. The optical micrographs are taken at several stages during the tensile test. Following the deformation process (*Figures 7a–d*) the size of the deformed region (whitened area) increases to a constant value ahead of the crack-tip. The whitened volume corresponds to the tensile toughness value as already discussed in reference 3.

Brittle-to-ductile transitions. In *Figure 3* brittle-to-tough transitions are clearly visible with increasing temperature or, at a constant temperature, with an increasing rubber concentration. The occurrence of a transition is indicated by a sudden increase of the notched tensile toughness. Inspection of the fractured samples provides an alternative independent determination of the critical situation. In *Figures 8a* and *b* micrographs of high-speed fractured notched tensile specimens are shown as observed in the ductile region. In principle the tensile specimens form a neck just below the fracture surface. The dimensions of the neck can be indicated by the values of d_1 and d_2 (*Figure 8b*). In particular the ratio d_1/d_2 represents the strain level locally at the fracture surface. Hence, via a comparison of the ratio d_1/d_2 of the various PS-PPE blends in the ductile region a qualitative insight can be obtained with respect to the influence of network density on the strain level just below the fracture surface of core–shell rubber-modified PS-PPE blends.

In *Figure 9* the ratio d_1/d_2 is plotted *versus* the rubber concentration for the various PS-PPE blends investigated at 75°C as a reference temperature because most data are present at this (high) temperature in the range of core–shell rubber percentages investigated. The brittle-to-ductile transitions are revealed by a rather abrupt increase of the ratio d_1/d_2. If the matrix ligament thickness is below the critical value, the strain-to-break of the material increases. It is interesting to notice that the strain level at the fracture surface (qualitatively) demonstrates the same network density dependence as the maximum

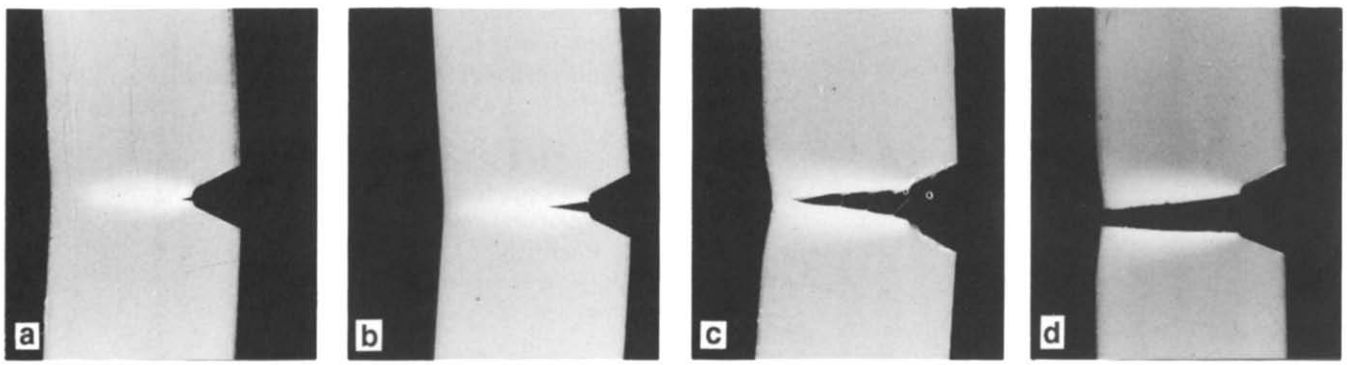

Figure 7 (a)–(d) Optical micrographs of slow-speed single-edge notched rubber-modified PS-PPE 20-80 blends taken at several stages of deformation

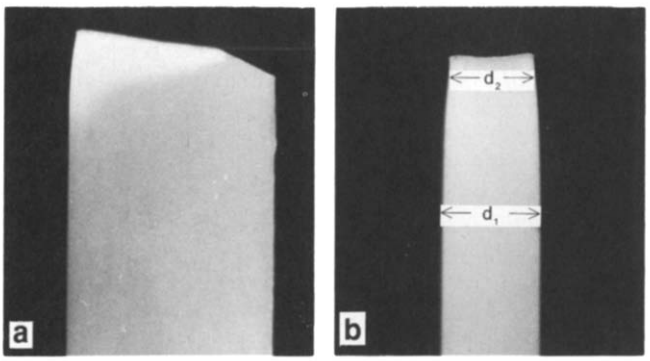

Figure 8 Micrographs of a high-speed fractured notched PS-PPE/*X* blend in the ductile region: (a) side view; and (b) edge-on view

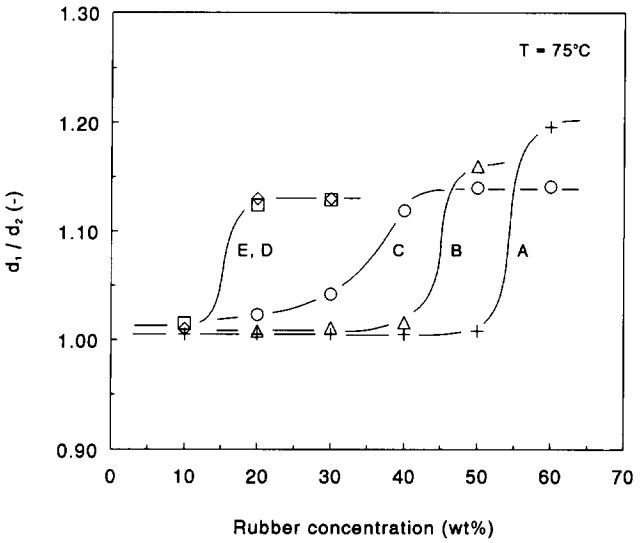

Figure 9 Deformation (d_1/d_2) of notched high-speed fractured PS-PPE blends *versus* rubber concentration with matrix composition (PS-PPE): (A) 100-0; (B) 80-20; (C) 60-40; (D) 40-60; and (E) 20-80 (reference temperature 75°C)

macroscopic strain-to-break listed in reference 2. PS (*Figure 9*, curve A) demonstrates the maximum ratio d_1/d_2 in the tough region, i.e. the highest strain level locally at the fracture surface similar to the highest strain-to-break level for PS reported in reference 2 during slow-speed uniaxial tensile testing of core–shell rubber-modified PS-PPE blends at room temperature. The addition of PPE results in a shift of the brittle-to-ductile transition to lower rubber concentrations, again, analogous to the conclusions derived during the discussion of the unnotched slow-speed measurements presented in part 2 of this series[2].

In order to compare the brittle-to-ductile transitions of the various PS-PPE blends as observed in *Figure 3* in a more convenient way, in *Figure 10* the normalized (relative to the value in the tough region) value of the tensile toughness is shown *versus* the rubber concentration at two reference temperatures (25°C and 75°C). For each PS-PPE composition, the value of the notched tensile toughness for a distinct rubber concentration is normalized to the highest recorded value of G_h at the given reference temperature. Only for the PS-PPE 40-60 and 20-80 blends can the brittle-to-ductile transition be determined at 25°C as a reference temperature. From *Figure 10* (or equally well from *Figure 9*) ID_c can be determined for the various PS-PPE blends assuming a body-centred-cubic lattice[9–11].

In *Figure 11* these values of ID_c as determined from a notched tensile test are shown as a function of the network density for the two different reference temperatures (25°C and 75°C). For comparison ID_c values, as determined during slow-speed uniaxial tensile testing at room temperature[2], are incorporated in *Figure 11*. The values of ID_c determined via slow-speed uniaxial tensile testing compare well with the ID_c data extracted from notched high-speed tensile testing. Apparently, within the investigated strain rate and temperature range the value of ID_c is rather insensitive to changes in testing speed and temperature as could be expected (*Figure 1*). The full curves in *Figure 11* represent the value of ID_c as a function of the network density as predicted by the simple model [see equation (1)], calculated for three different values of the yield stress (60, 70 and 90 MPa). These values of the yield stress are chosen rather arbitrarily since the yield stress in the ligament cannot simply be converted into a macroscopic yield stress due to the presence of the notch (see discussion after *Figure 3*). Especially in the region of low network densities, ID_c proves to be rather insensitive to changes in the yield stress, thus, it is relatively insensitive to changes in the testing speed or temperature.

The absolute value of the notched tensile toughness is not simply governed by the maximum strain-to-break but depends on the geometry of the specimen[12–17] and the quasi macroscopic effective yield stress (related to the volume fraction of holes). A quantitative prediction of G_h in the ductile region can only be made if the stress

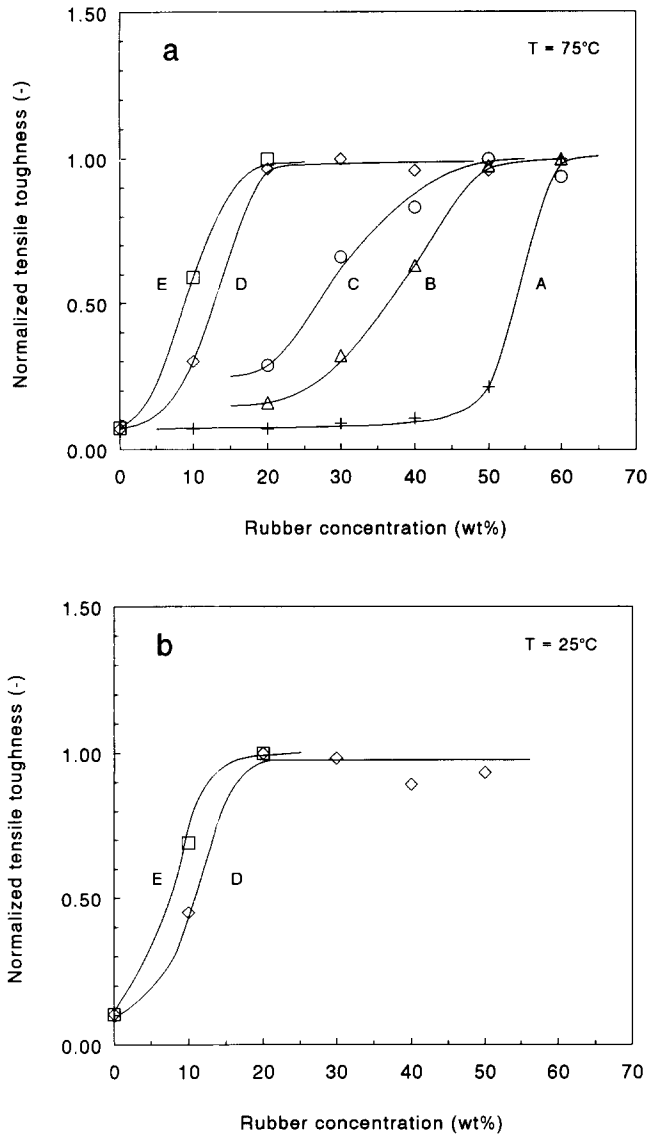

Figure 10 Normalized notched tensile toughness *versus* rubber concentration with matrix composition (PS-PPE): (A) 100-0; (B) 80-20; (C) 60-40; (D) 40-60; and (E) 20-80. Reference temperature: (a) 75°C; and (b) 25°C

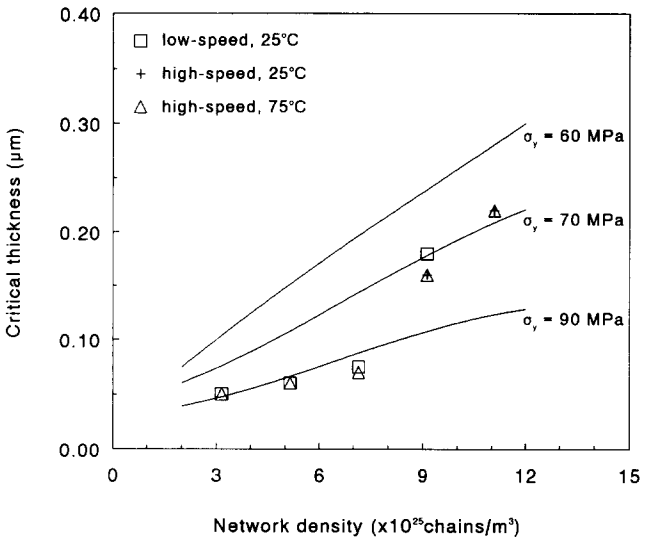

Figure 11 Critical matrix ligament thickness *versus* network density. The full curves are according to the model. For details see text

state behind the notch-tip is fully understood. Therefore, absolute values of G_h can only result from a full stress analysis. A multi-level finite element modelling of the test sample can result in a more quantitative description of the network density dependence of the value of the notched tensile toughness in the ductile region. This aspect is a major topic of the present research in our laboratory.

CONCLUSIONS

Tensile dilatometry at testing speeds of $1\,m\,s^{-1}$ (strain rate $10\,s^{-1}$) reveal that the deformation mechanism of PS in the ductile region ($ID \leqslant ID_c$) is shear deformation. The ID_c of PS as determined with uniaxial slow-speed tensile testing at room temperature proves to be valid up to testing speeds of $1\,m\,s^{-1}$ (strain rate $10\,s^{-1}$). A further increase of the local strain rate by the introduction of a razor-blade tapped notch results in a brittle fracture of the 60 wt% rubber-modified PS unless the increase in strain rate is compensated for by an increase in testing temperature to 70°C.

The influence of testing speed and temperature on the value of ID_c can be quantitatively understood in terms of the strain rate and temperature dependence of the yield stress (neglecting the strain rate and temperature dependence of the Young's modulus) using the simple model introduced in part 2 of this series, combined with an Eyring type of strain rate and temperature dependence of the yield stress.

Notched high-speed tensile testing of core–shell rubber-modified PS-PPE blends demonstrates that brittle-to-ductile transitions occur at about the same ID_c values as already determined during slow-speed uniaxial tensile testing at room temperature[2] provided that the testing temperature is increased. Apparently, the increase in yield stress, due to the local high strain rate as a consequence of the introduction of a notch, is counteracted by the increased temperature. The temperature dependence of ID_c according to the model is experimentally verified for PS-PPE 40-60 and 20-80 blends in a temperature range of 150°C up to 50°C below the T_g of the polymeric material.

ACKNOWLEDGEMENTS

The authors are indebted to F. O. de Bie and R. G. M. van Deursen for performing the notched high-speed tensile measurements. A. Schepens from DSM Research is acknowledged for his assistance in the injection moulding of several PS-PPE blends and L. E. Govaert is gratefully acknowledged for his assistance in the determination of the yield stress of PS for various strain rates. This research was financed by the Foundation for Polymer Blends (SPB).

REFERENCES

1 Van der Sanden, M. C. M., Meijer, H. E. H. and Lemstra, P. J. *Polymer* 1993, **34**, 2148
2 Van der Sanden, M. C. M., Meijer, H. E. H. and Tervoort, T. A. *Polymer* 1993, **34**, 2961
3 Van der Sanden, M. C. M. and Meijer, H. E. H. *Polymer* 1993, **34**, 5063

4 Eyring, H. *J. Chem. Phys.* 1936, **4**, 283
5 Kambour, R. P. *Polym. Commun.* 1983, **24**, 292
6 Govaert, L. E. unpublished data
7 Bucknall, C. B. 'Toughened Plastics', Applied Science, London, 1977
8 Narisawa, I., Kuriyama, T. and Ojima, K. *Makromol. Chem., Macromol. Symp.* 1991, **41**, 87
9 Borggreve, R. J. M., Gaymans, R. J., Schuijer, J. and Ingen Housz, J. F. *Polymer* 1987, **28**, 1489
10 Wu, S. *Polymer* 1985, **26**, 1855
11 Wu, S. *J. Appl. Polym. Sci.* 1988, **35**, 549
12 Kinloch, A. J. and Young, R. J. 'Fracture Behaviour of Polymers', Elsevier, London, 1985
13 Brown, H. R. *J. Mater. Sci.* 1982, **17**, 469
14 Yap, O. F., Mai, Y. W. and Cotterell, B. *J. Mater. Sci.* 1983, **18**, 657
15 Williams, J. G. 'Fracture Mechanics of Polymers', Ellis Horwood–Wiley, Chichester, 1984
16 Vincent, P. I. 'Impact Tests and Service Performance of Thermoplastics', Plastics Institute, London, 1971
17 Hertzberg, R. W. 'Deformation and Fracture Mechanics of Engineering Materials', John Wiley & Sons, New York, 1976